Cellular Physiology and Biochemistry

Cell Physiol Biochem 2014;34:790-803
DOI: 10.1159/000363043
Published online: August 19, 2014
Accepted: July 02, 2014

Karger Open access

1421-9778/14/0343-0790$39.50/0

Original Paper

L-Carnitine Reduces in Human Conjunctival Epithelial Cells Hypertonic-Induced Shrinkage through Interacting with TRPV1 Channels

Noushafarin Khajavi[a] Peter S. Reinach[b] Marek Skrzypski[c,d] Anja Lude[a] Stefan Mergler[a]

[a]Charité – Universitätsmedizin Berlin, Campus Virchow-Clinic, Department of Ophthalmology, Berlin, Germany, [b]School of Ophthalmology and Optometry, Wenzhou Medical University, Wenzhou, P.R.China, [c]Department of Hepatology and Gastroenterology & the Interdisciplinary Centre of Metabolism: Endocrinology, Diabetes and Metabolism, Charité-University Medicine Berlin, Berlin, Germany, [d]Department of Animal Physiology and Biochemistry, Poznań University of Life Sciences, Poznań, Poland

Key Words
Human conjunctival epithelium • L-carnitine • Transient receptor potential channels • Calcium • Osmoprotectants • Cell-volume • Planar patch-clamp technique • Capsaicin receptor

Abstract
Background/Aims: Ocular surface health depends on conjunctival epithelial (HCjE) layer integrity since it protects against pathogenic infiltration and contributes to tissue hydration maintenance. As the same increases in tear film hyperosmolarity described in dry eye disease can increase corneal epithelial transient receptor potential vanilloid type-1 (TRPV1) channel activity, we evaluated its involvement in mediating an osmoprotective effect by L-carnitine against such stress. ***Methods:*** Using siRNA gene silencing, Ca^{2+} imaging, planar patch-clamping and relative cell volume measurements, we determined if the protective effects of this osmolyte stem from its interaction with TRPV1. ***Results:*** TRPV1 activation by capsaicin (CAP) and an increase in osmolarity to ≈ 450 mOsM both induced increases in Ca^{2+} levels. In contrast, blocking TRPV1 activation with capsazepine (CPZ) fully reversed this response. Similarly, L-carnitine (1 mM) also reduced underlying whole-cell currents. In calcein-AM loaded cells, hypertonic-induced relative cell volume shrinkage was fully blocked during exposure to L-carnitine. On the other hand, in TRPV1 gene-silenced cells, this protective effect by L-carnitine was obviated. ***Conclusion:*** The described L-carnitine osmoprotective effect is elicited through suppression of hypertonic-induced TRPV1 activation leading to increases in L-carnitine uptake through a described Na^{+}-dependent L-carnitine transporter.

Stefan Mergler, PhD

Charité – Universitätsmedizin Berlin, Campus Virchow-Clinic
Department of Ophthalmology, Augustenburger Platz 1, 13353 Berlin (Germany)
Tel. +49 (030) 450 559648, E- Mail stefan.mergler@charite.de

Introduction

The conjunctival epithelial layer is essential for normal vision since its tight junctions are protected against pathogenic infiltration and are needed for this tissue to elicit sufficient osmotic-driven fluid flow to prevent desiccation of the ocular surface. Such regulation by this tissue contributes to maintaining normal tear film osmolarity and isotonic cell volume, which sustains close cell-to-cell apposition. However, functional conjunctival tissue activity is compromised by tear film hyperosmolarity described in some types of dry eye disease. This effect can contribute to the symptomology accompanying this disease. This realization of the importance of maintaining intracellular volume isotonicity with the external milieu to treat dry eye disease prompted efforts to identify osmolytes that could be of therapeutic value in countering presumed declines in corneal and conjunctival cell volume occurring in some types of dry eye disease. One of the organic osmolytes evaluated in dry eye mouse models, which improves ocular surface hydration is L-carnitine [1]. Its effectiveness stems from the fact that it is taken up into the cell interior by a Na^+ coupled co-transporter during exposure to a hypertonic stress and contributes to equilibrating the intracellular milieu with the external environment [2]. However, the identity of the epithelial hypertonic sensor activating the net uptake of L-carnitine during exposure is unknown.

In human conjunctival epithelial cells (HCjE), one of the transient receptor potential (TRP) channels in the 28 member TRP superfamily that is activated by an increase in osmolarity was identified by us. This subtype is TRPV1 (capsaicin receptor) [3]. Our evidence for functional TRPV1 expression in human conjunctival and corneal epithelial cells (HCjE and HCEC, respectively) includes showing that a selective TRPV1 agonist capsaicin (CAP) induces Ca^{2+} transients and underlying whole-cell currents that are eliminated by exposure to a TRPV1 antagonist, capsazepine [4]. Such expression is also evident in human corneal epithelial cells (HCEC) since exposure to a hypertonic stress elicits TRPV1 activation leading to increases in proinflammatory cytokine release via mitogen-activated protein (MAP) kinase and NF-κB signaling [5]. It has been suggested that TRPV1 may be a potential drug target to reduce dry eye symptomology since this receptor can be stimulated during exposure to the same hypertonic conditions identified in tear samples obtained from dry eye patients [6]. This consideration prompted us to hypothesize that the osmoprotective effects of L-carnitine against hypertonic-induced cell volume shrinkage are elicited through an interaction of this osmolyte with TRPV1 in a HCjE immortalized cell line (IOBA-NHC).

We describe here changes in intracellular Ca^{2+} regulation and whole-cell currents in IOBA-NHC cells induced by L-carnitine in the presence and absence of CAP. The association between these changes and the inhibitory effects of L-carnitine on hypertonic-induced cell volume shrinkage in the presence of functional TRPV1 expression suggest that its osmoprotective effect stems from its interaction with TRPV1. TRPV1 inhibition by carnitine appears to contribute to activation of a described Na^+ dependent L-carnitine transporter in this tissue during exposure to such a challenge since this osmolyte reversed CAP- as well as hypertonic-induced increases in $[Ca^{2+}]_i$ and also reduced CAP elicited rises in underlying whole-cell currents [2].

Materials and Methods

Cell Culture

The IOBA-NHC cell line was established through immortalization of normal human conjunctival epithelial cells and was kindly provided by Yolanda Diebold's lab. Cells were cultivated as previously described [7]. In brief, IOBA-NHC cells were grown in Dulbecco modified Eagle medium DMEM/HAMs F12 1:1 supplemented with 10% fetal calf serum (FCS), 1 µg/ml insulin, 5 µg/ml hydrocortisone and 100 IU/ml penicillin/streptomycin in a humidified 5% CO_2 incubator at 37°C.

RNA isolation and reverse transcriptase polymerase chain reaction (RT-PCR)

Total RNA was extracted from IOBA-NHC cells using TRIzol® Reagent RT (Ambion, Austin, TX). The isolated RNA (2 µg) was transcribed into cDNA using the High Capacity cDNA Reverse Transcription Kit (Applied Biosystems, Darmstadt, Germany). For reverse transcription PCR, 2 µl cDNA mixture was used as template in subsequent amplification reactions in a 30 µl total volume containing specific primers for TRPV1 (fwd CTCTGGTGGCTAGCCTGTCCTGACA; rev TGGGATCCCGGAGCTTCTCA) generating 285 bp and glyceraldehyde-3-phosphate dehydrogenase (GAPDH) as template control (fwd TCAACGACCACTTTGTCAAGCTCA; rev GCTGGTGGTCCAGGGGTCTTACT) generating a 119 bp product. Each reaction also contained red PCR Master Mix (Srtatec, Germany). PCR reaction underwent an initial cycle at 95 °C for 5 min followed by 35 cycles at 95 °C for 15 s, Primer specific annealing temperatures used were: a) TRPV1 58 °C, b) GAPDH 60 °C for 30 s, followed by 72 °C for 45 s, and elongation at 72 °C for 7 min and finally temperature holding at 4 °C. Eight microliters of a PCR product were loaded on a 1.5 % agarose gel and after electrophoresis it was visualized via ethidium bromide staining under UV light.

Quantitative real-time PCR

Real-time PCR was performed with Mx 3000P qPCR System real-time cycler (Stratagene, Waldbronn, Germany) using specific primers for TRPV1 (fwd TCGCCCTCATGGGTGAGACTGT, rev CACCTGCAGCAGCTTGCCTGA) generating a 149 bp product and LightCycler® 480 SYBR Green I Master (Roche, Germany) for detection. Amplification was carried out for 45 cycles of 15 s (95°C), 30 s (60°C) and was followed by TBE-buffered gel electrophoresis in a 1% agarose gel. Mean C_T values were calculated and for the relative quantification (RQ), the "relative" expression values were calculated from the delta delta C_T values. For the normalization, the housekeeping gene GAPDH served as an internal control.

Western blot

After adding RIPA buffer (50 mMol Tris–HCl, pH 8.0 with 150 mM NaCl, 1.0% NP-40, 0.5% sodium deoxycholate, 0.1% SDS, 10 mM NaF and 1 mM Na_3 VO_4) supplemented with protease inhibitor cocktail (Roche Diagnostics, Penzberg Germany) to the IOBA-NHC cells, they were scraped and incubated on ice for 10 min. Lysates were obtained by centrifugation at 14,000×g for 15 min at 4°C. Protein concentration was determined by BCA Protein Assay Kit (Thermo Scientific, Rockford, IL, USA). Briefly, proteins were isolated in a RIPA containing buffer.. Twenty five µg of protein were loaded, resolved on 12% Tris–HCl SDS-PAGE gel and blotted onto a nitrocellulose membrane (Amersham Biosciences, Freiburg, Germany). Membranes were blocked for 1 h using 5% bovine serum albumin at room temperature and incubated with primary rabbit polyclonal TRPV1 antibody (Alomone Labs, Jerusalem, Israel) diluted 1: 1000, at 4°C for 16 h. After washing, the membranes with PBS-T (3x 15 min), they were incubated with HRP-conjugated anti-rabbit secondary antibody (Dako, Hamburg, Germany) diluted 1: 5000 for 1 h at room temperature. Immunobound antibody was visualized with an enhanced chemiluminescence kit (GE Healthcare Europe, Freiburg, Germany). ChemiDoc MP Imaging System (BioRad) was used for chemiluminescence detection. For the loading control, membranes were incubated with antibody against ß-actin (Sigma Aldrich) diluted 1: 10000 for approximately 16 h at 4°C.

Immunocytochemistry

Cells seeded on glass coverslips were cultured at 37°C in a humidified 5% CO_2 incubator until they were 50 - 70% confluent. After washing the cells twice with PBS, they were fixed with 4% (w/v) paraformaldehyde in PBS for 20 min. Cells were rinsed twice with PBS and then rendered permeable using 0.1% Triton X-100 solution. After blocking with 10% BSA, cells were incubated overnight at 4°C with primary rabbit polyclonal TRPV1 antibody. Cells were twice washed with PBS and exposed to anti-rabbit secondary antibody for 1 h and mounted with DAPI for 5 min. Fluorescence was visualized with a Zeiss inverted microscope.

TRPV1 siRNA transfection

ON-TARGETplus SMART pool of four individual candidate TRPV1 siRNAs 1#: GGAGACUAUUUCCGAGUUA, 2#: UGACGAGCAUGUACAAUGA, 3#: CAUCUAUGCCGUCAUGAUA, 4#: CCCGAUAGCUCCUACAACA and non-targeting siRNA were obtained from Thermo Scientific Dharmacon (Waltham, MA, USA). Fast-Forward transfection with 50 nM non-targeting siRNA or 50 nM TRPV1 siRNA was performed using HiPerfect reagent (Qiagen, Germany), according to the manufacturer's protocol. Western blot and immunocytochemistry were

performed for detection of TRPV1 protein expression. The most effective incubation time for obtaining maximal suppression of TRPV1 protein expression was 48 h.

Fluorescence $[Ca^{2+}]_i$ measurement

Time dependent changes in cytosolic free $[Ca^{2+}]_i$ were monitored by measuring fura-2 fluorescence. Cells were preincubated in a culture medium containing 1 µM fura-2/AM for 30 min at 37°C. Thereafter, stained cells were rinsed in a Ringer-like solution containing 150 mM NaCl, 6 mM CsCl, 1.5 mM $CaCl_2$, 1 mM $MgCl_2$, 10 mM HEPES acid and 10 mM glucose (pH~7.4) (osmolarity ≈ 300 mOsM). Fluorescence measurements were performed at room temperature on the stage of an inverted microscope (Olympus BW50WI) with a digital imaging system (TILL Photonics, Munich, Germany). For evaluation, TIDA software was used (HEKA electronics, Lamprecht, Germany). Fura-2 fluorescence was alternately excited at 340 and 380 nm wavelength and emission was detected every 500 ms at 510 nm. The measuring field contained a cluster of fura-2-loaded cells. The fluorescence ratio ($f_{340\ nm}/f_{380\ nm}$) is a relative index of changes in $[Ca^{2+}]_i$ [8]. Results are mean traces f_{340}/f_{380} ± SEM with n values indicating the number of experiments per data point. The measurements lasted between 8 to 10 min depending on the experimental design.

Planar patch-clamp recordings

The semi-automated planar patch-clamp technique in conjunction with an EPC10 amplifier and the acquisition software PatchMaster (HEKA, Lambrecht, Germany) as well as the PatchControl software (Nanion, Munich, Germany) were used to obtain and evaluate electrophysiological recordings [9]. The resistance of the chips corresponded to those of a patch-pipette with a resistance of 3-5 MΩ. For recording, first of all, 5 µl of an internal-like solution contained in mM: 50 CsCl, 10 NaCl, 2 $MgCl_2$, 60 CsF, 20 EGTA and 10 HEPES (pH 7.2; osmolarity ≈ 288 mOsM) was applied to the microchip. Cs in the internal solution blocks potassium channel outward currents, and the fluoride hydrate-covering suppresses possible anion chloride channels. Thereafter, a single cell suspension was prepared in external solution whose composition was (in mM): 140 NaCl, 4 KCl, 1 $MgCl_2$, 2 $CaCl_2F$, 5 D-glucose monohydrate and 10 HEPES (pH ≈ 7.4; osmolarity ≈ 298 mOsM). Suction was applied automatically by a software controlled pump in order to move a single cell on to the aperture of the microchip. Additional suction pulses were used to break open the cell membrane establishing the whole-cell configuration. The holding potential (HP) was set to 0 mV to eliminate any possible contributions by voltage-dependent Ca^{2+} or Na^+ channel activity. Whole-cell currents were recorded using a step protocol involving voltage steps of 10 mV ranging between -60 to +130 mV for 400 ms. Voltage changes without steps (voltage ramp) were also used. Membrane capacitance and access resistance were calculated with Patchmaster software. A mean access resistance R_S of 61 ± 13 MΩ (n = 8) and a mean membrane capacitance C_M of 8 ± 1 pF (n = 8) were observed in the whole-cell configuration. Series resistance errors as well as fast and slow capacity transients were compensated by the software controlled patch-clamp amplifier. Cells with leak currents above 100 pA were discarded and current recordings were leak-subtracted. All plots were generated with SigmaPlot software version12.3 (Systat, San Jose, California, U.S.A.) and an electrophysiology module (Systat, Bruxton).

Relative cell volume measurements

Relative cell volume was evaluated in a fluorescence microplate analyzer. IOBA-NHC cells were plated in a black 96-well culture plate and grown to 80 to 90% confluence. After washing the cells twice with PBS, they were loaded with the volume-sensitive fluorescence dye 50 µg calcein/AM dissolved in 25 µl DMSO (Invitrogen, Karlsruhe, Germany) whose stock concentration was 2 mM. IOBA-NHC cells were incubated for 1 h with 1 µM calcein/AM and then washed again twice with PBS and incubated at room temperature with isotonic Ringer-like solution containing L-carnitine for 30 min. Relative cell volume measurements were performed using a VICTOR™ X Multilabel Plate Reader (Htds, Paris, France). Calcein fluorescence was excited at 485 nm and emission was detected at 530 nm with an integrated photometry system. Bleaching was minimized by exciting calcein every 30 s. A 5 min isotonic baseline was recorded each time prior to a hypertonic challenge. Before each experiment, fluorescence intensity was monitored under isotonic conditions and used for the calculation of drift correction.

Data analyses and statistics

Parametric paired Student's *t*-test was used and in case of too much variance; unpaired *t*-test with Welch's correction was used. P values < 0.05 (*) were considered as significant. If normality test failed,

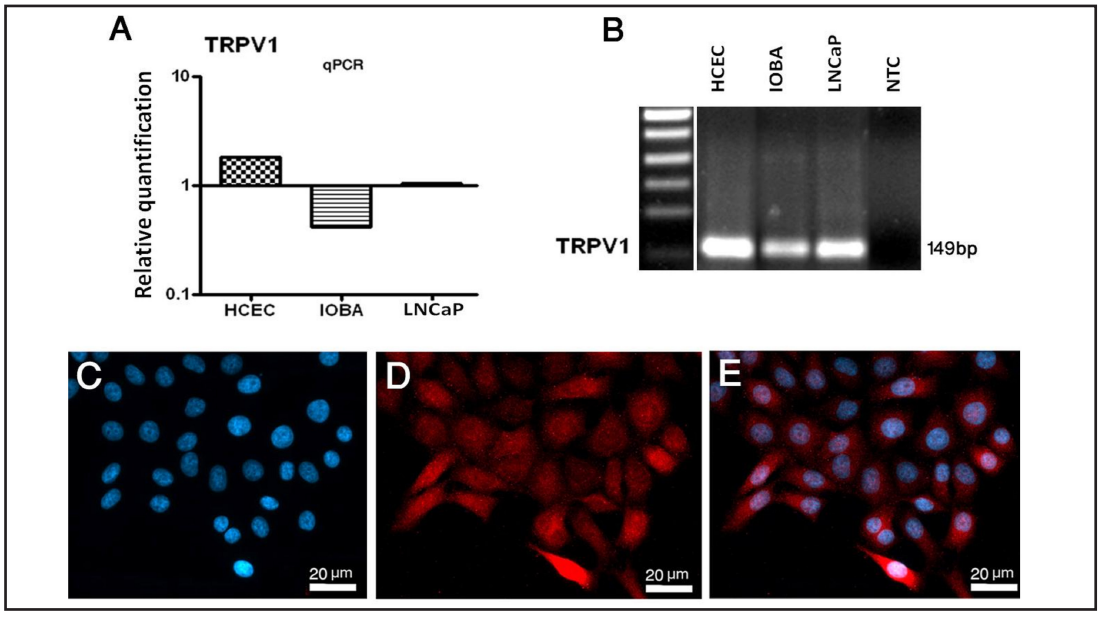

Fig. 1. TRPV1 gene and protein expression in IOBA-NHC cells. A: Conventional RT-PCR indicate mRNA signal of TRPV1 (285 bp) in HCEC-12 (human corneal endothelial cells), LNCaP (lymph node carcinoma of prostate) and IOBA-NHC (normal human conjunctival). The data were normalized to LNCaP with the positive mRNA signal. No template control (NTC) proved no template contamination. B-D: Immunocytochemistry shows TRPV1 localization. B: Staining nucleus with DAPI (blue). C: TRPV1 positive cells (red). D: merged.

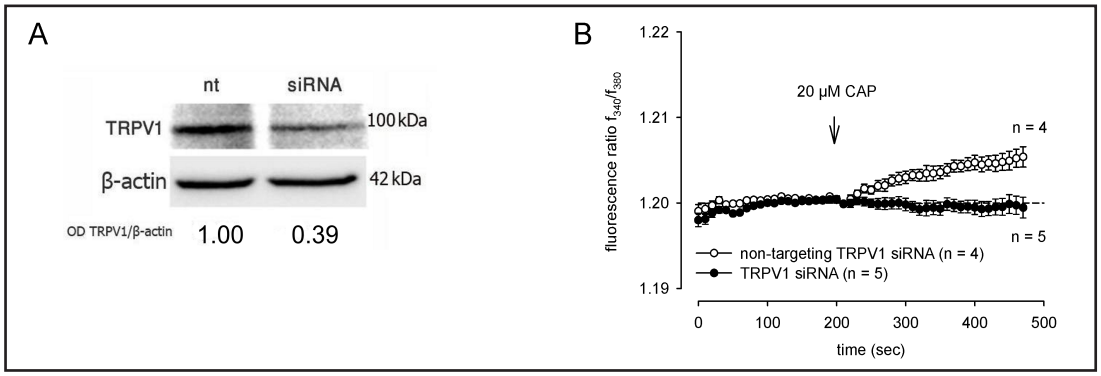

Fig. 2. TRPV1 siRNA led to a strongly reduced TRPV1 protein expression and abolished CAP-induced Ca^{2+} increase. A: Western blot showing reduced level of TRPV1 protein expression (100 kDa). ß-actin was used as a house keeping gene (42 kDa). A control experiment validating anti TRPV1 antibody selectivity was performed using a TRPV1 expressing tumor cell line as a positive control (data shown in [10]). B: Fluorescence Ca^{2+} imaging data clearly confirmed functional expression of TRPV1 (20 µM CAP; open circles) since CAP did not increase Ca^{2+} in TRPV1 siRNA treated IOBA-NHC cells (filled circles).

nonparametric Wilcoxon rank sum test was used. Statistical analysis was performed with GraphPad Prism (GraphPad software Inc, (La Jolla, CA, U.S.A.) and SigmaPlot software and the values are reported as means ± SEM.

Results

TRPV1 gene and protein expression in human conjunctival epithelial (HCjE) cells

TRPV1 gene expression (285 bp) was identified in IOBA-NHC cells using both RT-PCR (Fig. 1A) and quantitative real-time PCR analysis. Interestingly, immunofluorescence staining revealed with a previously validated selective anti TRPV1 antibody TRPV1 protein expression that it is not plasma membrane delimited, but also found in the cytoplasmic region (Figs.

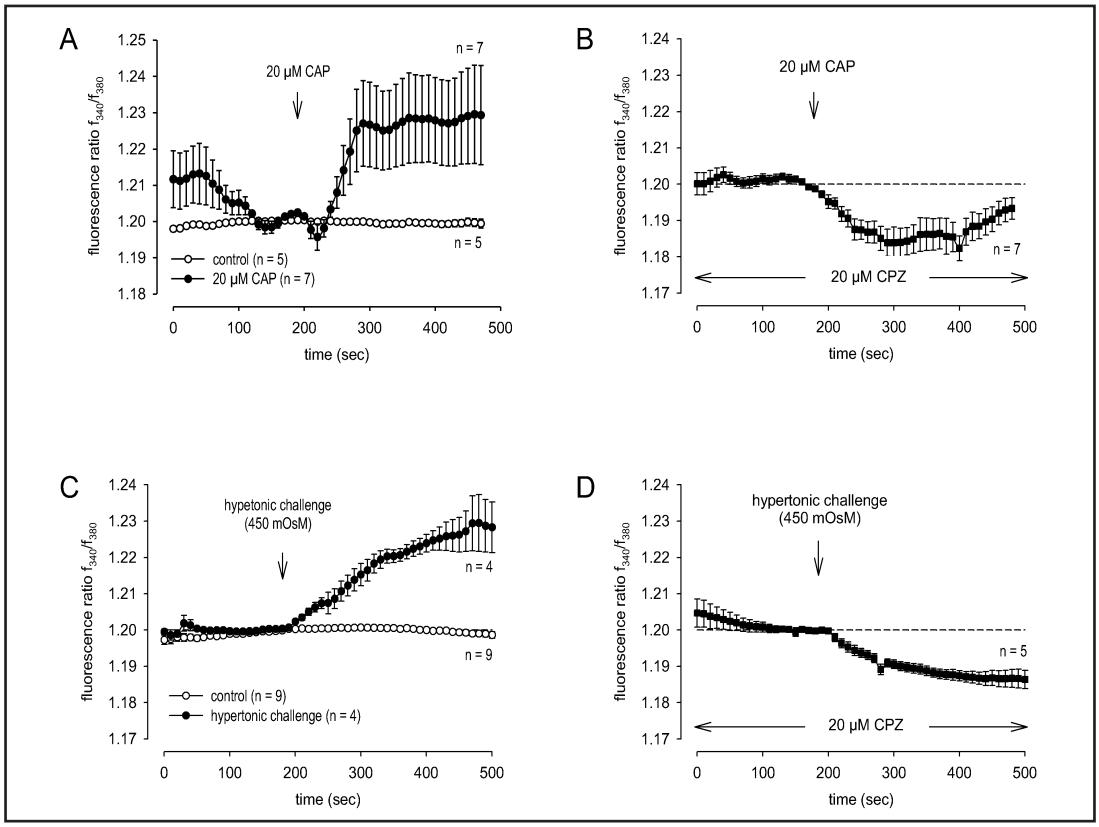

Fig. 3. Capsaicin (CAP) and hyperosmolarity increased Ca^{2+} influx in IOBA-NHC cells and capsazepine (CPZ) blocks this effect. A: 20 µM CAP induced an irreversible Ca^{2+} entry (n = 7; filled circles). Without CAP application, no changes in Ca^{2+} influx could be observed (n = 5; open circles). B: 20 µM CPZ suppressed the CAP-induced Ca^{2+} influx (n = 7). C: Hyperosmotic stress (450 mOsM) also increased Ca^{2+} influx (n = 4; filled circles) whereas no Ca^{2+} entry could be detected without the application of hyperosmotic stress (n = 9; open circles). D: 20 µM CPZ suppressed Ca^{2+} influx induced by hyperosmotic stress (n = 5). Moreover, even a reduction below baseline could be observed similar as shown in Fig. 3B.

1D-E). Validation is based on the western blot analysis demonstrated in a tumor cell line a single band of apparent molecular weight corresponding to TRPV1 [10]. Figure 2A compares in equal protein containing aliquots TRPV1 expression in IOBA-NHC cells transfected with irrelevant siRNAs and those transfected with relevant siRNAs. As found previously, TRPV1 expression level declined by 61% in TRPV1 siRNA transfected cells whereas in wildtype cells transfected with irrelevant siRNAs the expression level was unchanged from that in the non-transfected counterpart [10].

Functional expression of TRPV1

To assess TRPV1 function in HCjE cells, the effects were measured of a relatively selective TRPV1 agonist, capsaicin (CAP; 20 µM) on intracellular Ca^{2+} levels. Figure 3A shows that CAP induced an irreversible increase in the f_{340}/f_{380} ratio from 1.205 ± 0.0003 (baseline value, t = 150 s) to 1.228 ± 0.012 (n = 7; *< 0.05; t = 350 s). After 450 s, this ratio was at the same level (1.2291 ± 0.013; n = 7; *< 0.05). Preincubation with the relatively selective TRPV1 channel blocker capsazepine (CPZ; 20 µM) negated the rise in $[Ca^{2+}]_i$ (Fig. 3B).

Hyperosmotic challenge elicits TRPV1 activation

Figures 3C and D show the differential effects of exposure to 450 mOsM on $[Ca^{2+}]_i$ in the presence and absence of 20 µM CPZ. Without CPZ, $[Ca^{2+}]_i$ gradually and irreversibly rose from 1.200 ± 0.00125 (t = 180 s) to 1.240 ± 0.020 (t = 500 s) (n = 5; * p < 0.05) whereas with

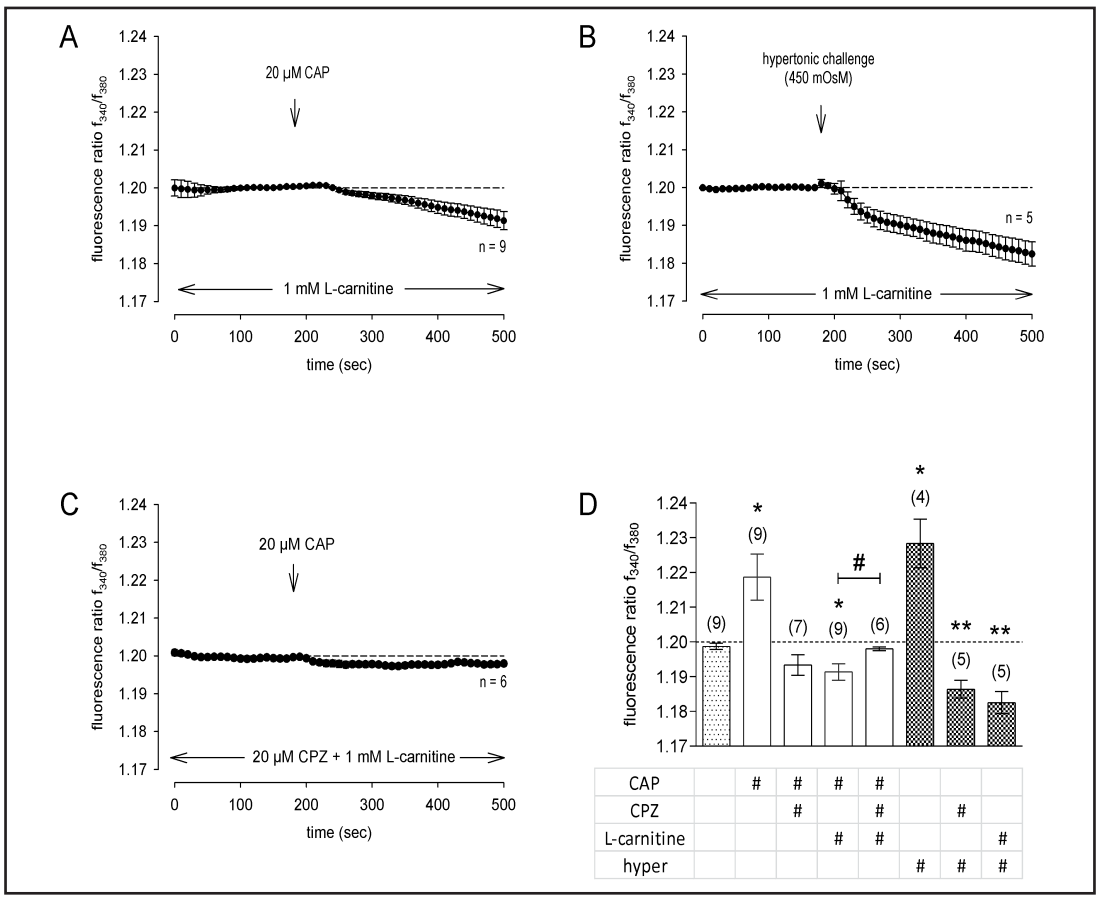

Fig. 4. L-carnitine inhibits CAP and hyperosmotic stress-induced Ca^{2+} influx in IOBA-NHC cells. A: 20 µM CAP induced Ca^{2+} entry could be completely suppressed with 1 mM L-carnitine preincubation (filled triangles). Moreover, even a reduction below baseline could be observed. As the negated rise in $[Ca^{2+}]_i$ was similar as CPZ in the previous set of experiments, it is suggested that L-carnitine may influence the TRPV1-mediated Ca^{2+} regulation. B: Similarly, a Ca^{2+} increase by hypertonic challenge could be completely suppressed with 1 mM L-carnitine preincubation (filled triangles). A reduction below baseline could also be observed similar to that shown in Fig. 4A. C: In contrast, no reduction below baseline could be observed if cells were preincubated in both 20 µM CPZ and 1 mM L-carnitine. D: Summary of the experiments with CAP, CPZ, L-carnitine and hypertonic challenge. The asterisks (*) indicate significant differences (at the minimum $p < 0.05$; unpaired Student's t-test) between control (Ca^{2+} base level at 500 s) and 20 µM CAP, 20 µM CPZ, 1 mM L-carnitine and hypertonic challenge (450 mOsM), respectively (all at 500 s). The hash (#) indicates a significant difference ($p < 0.05$; unpaired Student's t-test) between CAP with CPZ and CAP with both CPZ and L-carnitine.

20 µM CPZ $[Ca^{2+}]_i$ it instead declined below the control level to reach 1.186 ± 0.0025 (n = 5; **$p < 0.01$). This effect shows that TRPV1 activation contributes to the rises in $[Ca^{2+}]_i$ induced by a hyperosmotic challenge (Fig. 3D, 4D).

Effect of L-carnitine on TRPV1-mediated Ca^{2+} regulation

The reversal of the rise in $[Ca^{2+}]_i$ induced by either CAP or a hypertonic challenge in the presence of CPZ suggested TRPV1 involvement in osmotic-induced cell shrinkage. As L-carnitine is an osmolyte countering hypertonic-induced corneal and conjunctival epithelial shrinkage through its uptake by a Na^+ dependent co-transporter, we determined if its protective effect involves a change in TRPV1 function [2]. We first evaluated TRPV1 involvement in eliciting the L-carnitine osmoprotective effect by seeing if the increases in $[Ca^{2+}]_i$ elicited by either CAP or a 450 mOsM challenge are altered in the presence of 1 mM

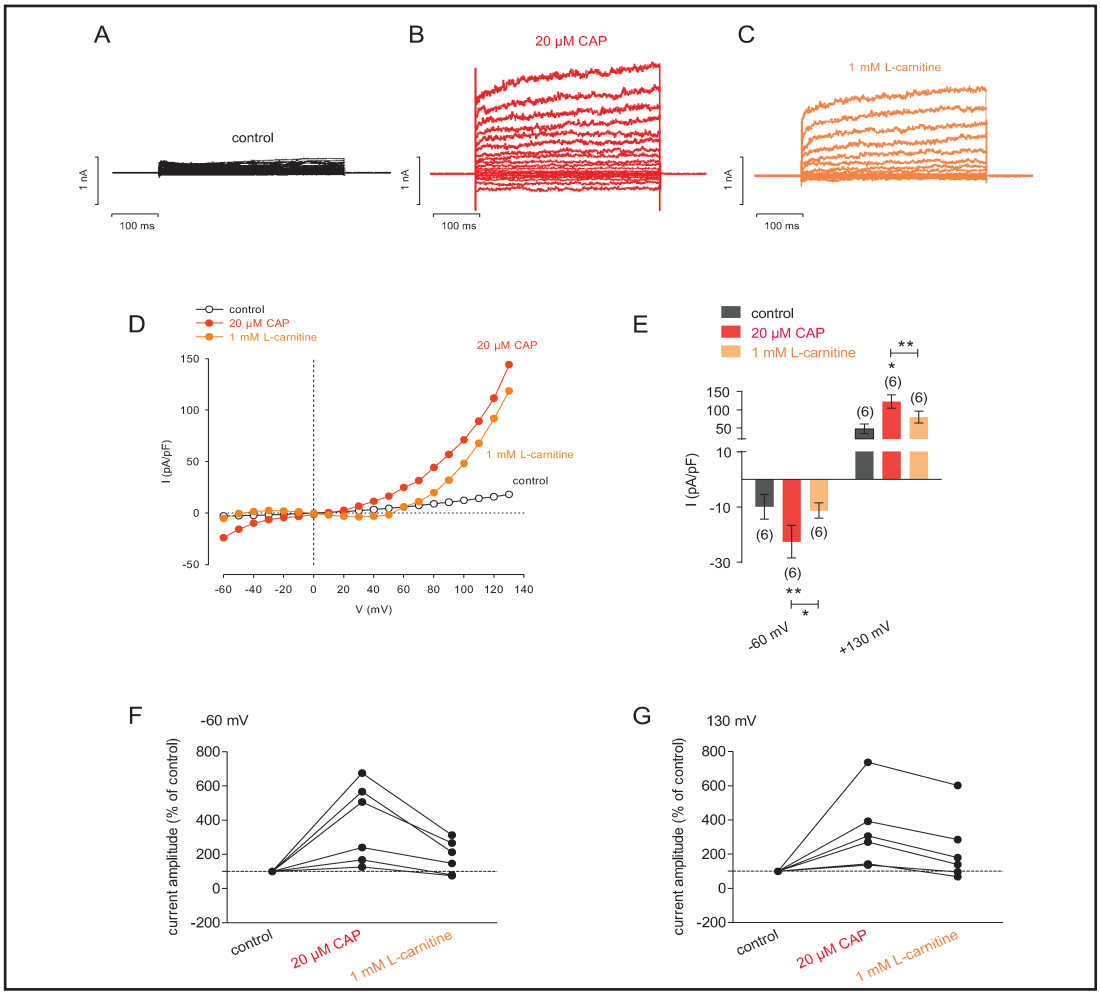

Fig. 5. Effect of CAP and L-carnitine on whole-cell currents. Currents were measured using the planar patch-clamp technique with leak subtraction. Holding potential was set to 0 mV to avoid influence of voltage dependent Ca^{2+} and Na^{+} currents A-B: Whole-cell currents following voltage stimulation from -60 to +130 mV in 10 mV steps for 400 ms each. 20 µM CAP increased in- and outward whole-cell channel currents. C: 1 mM L-carnitine suppressed both in- and outward currents. D: Effects of CAP and L-carnitine are summarized in a current/voltage plot (I/V plot). For the current/voltage relation, maximal peak current amplitudes were plotted against the voltage (mV). The upper trace (red filled circles) was obtained in the presence of 20 µM CAP and the lower trace (orange filled circles) in the presence of 1 mM L-carnitine. Controls without application of drugs had no effect on whole-cell currents (open circles). E: Summary of the experiments with CAP and L-carnitine (n = 6). The asterisks (*) indicate statistically significant differences of in- and outward currents with and without L-carnitine (n = 6; $p < 0.05$; paired tested). F: Maximal negative current amplitudes induced by a voltage step from 0 mV to -60 mV are depicted in percent of control values before application of 20 µM CAP. CAP-induced inward currents could be clearly suppressed in the presence of 1 mM L-carnitine. G: Maximal positive current amplitudes induced by a voltage step from 0 mV to 130 mV are depicted in percent of control values before application of 20 µM CAP. CAP-induced outwardly rectifying currents could be clearly suppressed in the presence of 1 mM L-carnitine.

L-carnitine. Figure 4A shows that preincubation with 1 mM L-carnitine for 15 to 60 min in isotonic medium had the same effect as CPZ on the hypertonic challenge; namely, a reversal of the increases in $[Ca^{2+}]_i$ induced by 20 µM CAP. Under this condition, baseline $[Ca^{2+}]_i$ fell from 1.200 ± 0.00056 to 1.191 ± 0.002 (n = 9; * $p < 0.05$; t = 500 s) (Fig. 4A). As with CAP, a hypertonic challenge also caused $[Ca^{2+}]_i$ to decline (Fig. 4B). The fluorescence ratio decreased

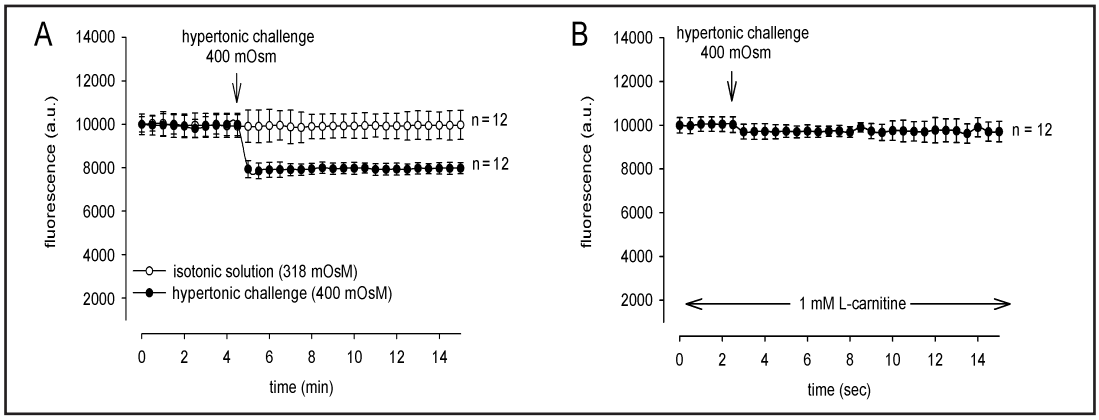

Fig. 6. L-carnitine suppresses hypertonocity-induced cell shrinkage. A: Hypertonic challenge (400 mOsM) led to a reduction of fluorescence signals corresponding to a reduction in the cell volume (filled circles). In contrast, isotonic solution (318 mOsM) had no effect (both n = 12; open circles). B: L-carnitine abolished the hypertonicity induced cell shrinkage (n = 12).

from 1.201 ± 0.001 (n = 5; t = 180 s) to 1.182 ± 0.003 (t = 500 s) in the presence of L-carnitine following hypertonic challenge (n = 5; ** $p < 0.01$). This equivalence between the inhibitory effects of L-carnitine and CPZ on the $[Ca^{2+}]_i$ transients induced by CAP and a hypertonic challenge suggests that L-carnitine and CPZ elicit $[Ca^{2+}]_i$ reversal through interacting with TRPV1. These reversal effects by 1 mM L-carnitine supplementation prompted us to hypothesize that L-carnitine elicits an osmoprotective effect against a hypertonic challenge through inhibition of TRPV1 activation. To test this hypothesis, we preincubated the cells with 20 μM CPZ and 1 mM L-carnitine and then exposed them to CAP. Under this condition, the results shown in Figure 4C indicate that the decline in $[Ca^{2+}]_i$ induced by CAP was less than that in the absence of L-carnitine (Fig 3B) suggesting that L-carnitine interaction with TRPV1is different than that of this antagonist.

Effect of L-carnitine on TRPV1-mediated whole-cell currents

To characterize the ionic currents underlying this L-carnitine-induced decline in intracellular Ca^{2+} levels, the planar patch-clamp technique in the whole-cell configuration was used (Fig. 5A-E). At -60 mV, CAP strongly increased inward currents from -10 ± 4 pA/pF to -23 ± 6 pA/pF confirming Ca^{2+} influx (n = 6; ** $p < 0.01$). At +130 mV, outwardly rectifying currents significantly increased from 48 ± 13 pA/pF to 122 ± 18 pA/pF in the presence of CAP (n = 6; * $p < 0.05$) (Fig. 5A-B). In contrast, in- and outward currents were significantly reduced in the presence of 1 mM L-carnitine in the external solution. Inward currents corresponding to the Ca^{2+} influx significantly decreased to -11 ± 3 pA/pF (n = 6; * $p < 0.05$) (Fig. 5C-E). Similarly, outwardly rectifying currents decreased to 80 ± 16 pA/pF (n = 6; ** $p < 0.01$) (Fig. 5C-E). In summary, L-carnitine clearly suppressed increases in whole-cell currents mediated by TRPV1 activation.

Effect of L-carnitine on cell volume regulation

The effects of L-carnitine on relative cell volume were monitored in calcein-AM loaded cells under optical conditions in which there is an inverse relationship between relative increases in cell volume and fluorescence intensity. Figure 6 A and B compares the effect of a hypertonic challenge on the fluorescence intensity in the presence and absence of 1 mM L-carnitine. To avoid irreversible shrinkage induced by 450 mOsM exposure, which prevented restoration of isotonic volume upon re-exposure to isotonic medium, the cells were exposed instead to 400 mOsM. This stress caused the signal to decline by ≈ 20% without any recovery (Fig 6A, filled circles). This decline is indicative of shrinkage due to dye quenching. On the other hand, Fig. 6B shows that during 1 mM L-carnitine exposure, the signal remained

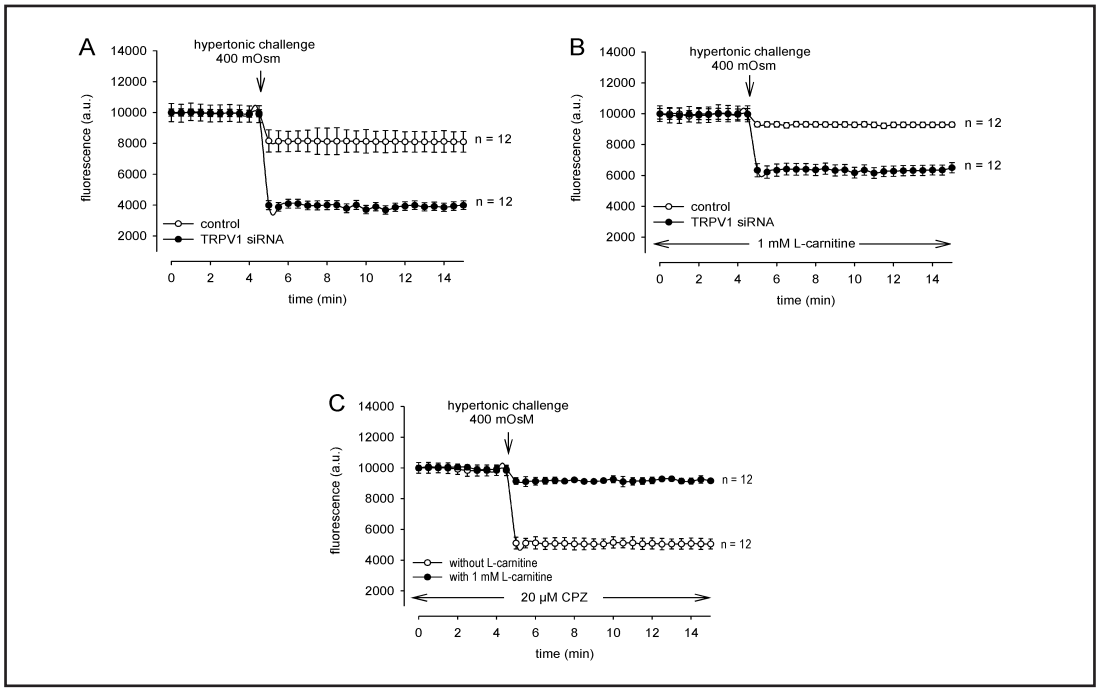

Fig. 7. L-carnitine effect is associated with TRPV1. A: TRPV1 siRNA treated cells (filled circles) led to a reduction of the cell volume at larger levels compared to controls (both n = 12; open circles). B: Same experiment as shown in A, but in cells pre-incubated in 1 mM L-carnitine. This clearly reduced the hypertonicity induced reduction in cell volume. C: Hypertonic challenge-induced cell shrinkage with L-carnitine (filled circles) and without L-carnitine (open circles) in cells preincubated in 20 µM CPZ.

unchanged suggesting that this osmolyte is internalized to equilibrate extracellular and intracellular osmolarity. To assess the involvement of TRPV1 in this osmoregulatory response to a hypertonic challenge, we determined whether L-carnitine in TRPV1 gene silenced cells affected the decline in fluorescence intensity induced by exposure to a hypertonic challenge. Figure 7A (open circles) shows again that in control non transfected TRPV1 expressing cells, the hypertonic challenge induced a 20% decline in fluorescence intensity whereas in TRPV1 gene silenced cells the signal declined instead by 65% (Fig. 7A, filled circles) suggesting a much larger cell volume shrinkage. On the other hand, preincubation with 1 mM L-carnitine in these gene-silenced cells was reduced to 40% suggesting that partial TRPV1 knockdown (i.e. 40%) was sufficient to induce partial protection against this challenge. The best protection against shrinkage was obtained in non-transfected cells exposed to both CPZ and L-carnitine since there was no perceptible shrinkage (Fig. 7C, filled circles). These results suggest that the osmosensor function of TRPV1 in eliciting a regulatory volume response depends on its inactivation leading to compensatory increases in L-carnitine uptake and equilibration with the external milieu.

Discussion

L-carnitine is reported to have osmoprotective effects against exposure to hypertonic stress in human corneal epithelial cells as well as in retinal pigment epithelial cells [11, 12]. However, an interaction was not considered between this osmolyte and TRPV1 in inducing an osmoregulatory response even though this channel acts as an osmosensor of hypertonic stress in numerous other tissues [3]. As there is TRPV1 gene- and protein expression as well functional activity in HCjE [7], we determined here if such an interaction exists in IOBA-NHC cells. We found that L-carnitine suppressed CAP-induced Ca^{2+} increases and whole-

cell currents. Furthermore, such effects of L-carnitine were associated with declines in TRPV1 function since hypertonic-induced shrinkage was less pronounced in TRPV1 gene silenced cells than in their non-transfected counterpart. A more definitive indication of the dependence of the osmoregulatory protective effect on TRPV1 inhibition is that relative cell volume was nearly invariant in non-transfected cells during exposure to either L-carnitine or CPZ (Fig. 7B and 7C, respectively).

Carnitine interaction with capsaicin receptor expression

TRPV1 protein expression was identified in both the plasma membrane and cytoplasmic regions. Its plasma membrane localization is consistent with CAP-induced increases in Ca^{2+} influx as well as suppression of this response by CPZ. Another indication is that in TRPV1 knockdown cells, CAP-induced Ca^{2+} influxes could be clearly suppressed despite a decline in TRPV1 protein expression of only approx. 60%. However, the functional role of cytosolic TRPV1 localization remains unclear. The reversal by L-carnitine of the rise in $[Ca^{2+}]_i$ induced by CAP and a hypertonic challenge (Fig. 4) suggested that this osmolyte induced a cellular osmoregulatory response countering shrinkage through suppressing TRPV1 function. A described Na^+ dependent: L-carnitine co-transporter in corneal and conjunctival epithelial cells is one mediator of L-carnitine's osmoprotective function [2]. To assess if L-carnitine uptake could contribute to osmoprotection against a hypertonic challenge in the presence of CPZ, we compared the effects of a hypertonic challenge on $[Ca^{2+}]_i$ in the presence and absence of L-carnitine. Figure 4 shows that the decline in $[Ca^{2+}]_i$ in the presence of L-carnitine was comparable to that of CPZ (Fig. 3B, 3D) indicating that intracellular Ca^{2+} regulation was similar during L-carnitine exposure. This suggests that L-carnitine provides an osmoprotective function against an intracellular Ca^{2+} rise induced by a hypertonic challenge. Even though there is sufficient evidence indicating that carnitine inhibits TRPV1 activation by either a hyperosmolar challenge or CAP, it is not possible to determine if its effect stems from an interaction with TRPV1 that is similar with CPZ. Nevertheless, it is possible that the critical channel determinants may be different for CPZ and L-carnitine since the declines in Ca^{2+} influx induced by CAP were less in the combined presence of both L-carnitine and CPZ than without L-carnitine. The mechanism of suppression of TRPV1 activation by capsazepine has been described in earlier studies. Critical molecular determinants located in the transmembrane domain between the third and fourth spans are required for capsazepine and other antagonists to prevent capsaicin from inducing TRPV1 activation. Our study did not employ the needed protocols and techniques to determine if L-carnitine also interacts with the same critical determinants described for a number of other structurally diverse antagonists [13].

L-carnitine and TRPV1 channels

While there are reports describing the effect of L-carnitine on Ca^{2+} channels in other tissues, to the best of our knowledge nothing is yet known about an interaction with TRP-like whole-cell currents. Some studies focused on voltage-operated Ca^{2+} channels (L-type) in porcine ventricular sarcolemma using palmitoyl-L-carnitine. Whereas at low concentrations (1 μM), L-type channel currents increased, they decreased at higher concentrations (10 μM) [14]. In another study in rat pheochromocytoma (PC12) cells, short-term exposure to 1 mM acetyl-L-carnitine ester instead decreased the open probability of L-type channels corresponding to lower L-type channel activity [15]. In our study, we used L-carnitine at a relatively higher concentration of 1 mM, than that in the L-type channel studies, but it was 10 times lower than that used in a human corneal epithelial cell line [12]. Our results show that L-carnitine clearly suppressed CAP-induced whole-cell currents. The properties of the CAP-induced currents correspond to those reported in this cell line [7]. TRPV1-like currents have an outwardly rectifying component and a reverse potential of 0 mV, which is indicative of non-selective ion channel currents. Notably, the CAP-induced Ca^{2+} inward currents (Fig. 5) are in line with CAP-induced Ca^{2+} influx. This is attributable to a high Ca^{2+} concentration in the external solution and a Ca^{2+} free internal solution that establishes a large inward directed

Ca^{2+} gradient. Under control conditions, there are nearly no inward currents, but only small outward currents, which probably are anion channel currents (chloride channels). Activation of chloride channels by CAP can be excluded since CAP is selective for TRPV1, which is a non-selective cation channel [16]. Therefore, it is suggested that these currents are mainly cation channel currents since similar studies in HCEC showed that with CAP increases in cation channel currents persisted even though chloride was replaced by gluconate [4]. As L-carnitine suppressed both of these currents, these declines stem from an inhibition by L-carnitine of TRPV1 function. Overall, the suppression by L-carnitine of CAP-induced increases in whole-cell currents are comparable to those elicited by CPZ in non-conjunctival epithelial cells [17].

L-carnitine and cell volume regulation

The hyperosmolar induced increases in Ca^{2+}influx mediated by TRPV1 channel activation are similar to those described in HCEC [5]. The fact that in the current study these increases in Ca^{2+}influx were attenuated by ≈ 65 % in TRPV1 knockdown cells substantiates the notion of TRPV1 involvement in inducing a Ca^{2+} transient. This indicates TRPV1 involvement in eliciting osmoregulatory responses to a hypertonic challenge by reducing shrinkage. L-carnitine practically blocked shrinkage induced by such a challenge through a presumable increase its intracellular uptake by a described L-carnitine Na^+ coupled co-transporter. This suggestion is consistent with our finding that in a Na^+-free medium L-carnitine had less of an effect on hypertonic-induced relative cell volume shrinkage (data not shown).

Potential clinical relevance

Currently, the treatment of dry eye disease is largely palliative since the underlying mechanisms of this sight compromising syndrome are not yet fully understood. In some types of dry eye disease arising from either decreases in tear volume secretion or increases in tear evaporation, there are reports that the tears are hypertonic [14]. In some cases in which there is extensive damage to the ocular surface caused by hypertonic-induced cell shrinkage and compromise of epithelial barrier function, tear film osmolarity increases can reach levels approaching those used in the current study [18]. Our results extend previous studies which showed in evaporative dry eye mouse models that osmolyte supplementation of artificial tears markedly improves ocular surface health by reducing inflammation and neovascularisation [1]. One of the osmolytes identified to have this therapeutic effect is L-carnitine since its intracellular uptake is stimulated during exposure to a hypertonic stress resulting in decreases in dry eye symptomology caused by cell volume shrinkage. The current study extends our understanding of the mechanism involved in eliciting activation of a described Na^+ coupled L-carnitine co-transporter whose activation elicits equilibration of the intracellular milieu with the extracellular osmolarity. The results indicate that TRPV1 by acting as a hypertonic osmosensor appears to elicit increases in L-carnitine uptake to reduce shrinkage. Interestingly, its role is dependent on TRPV1 inhibition by L-carnitine rather than activation. Taken together, these results suggest that it may be possible in a clinical setting to reduce hyperosmotic-induced ocular surface damage by blocking TRPV1 activation. Development of drugs for such a purpose may, however, be problematic since TRPV1 activation subsequent to injury has other functions that are essential to promoting wound healing by stimulating epithelial proliferation which is required for rapid closure of a wound [19, 20].

In summary, L-carnitine has an osmoprotective effect in HCjE cells because of its inhibitory effect on TRPV1-mediated Ca^{2+} signaling eliciting an osmoprotective effect against a hypertonic challenge. Studies are still needed to clarify how a decline in TRPV1 activity leads to activation of Na^+ dependent L-carnitine co-transporters and equilibration of the intracellular and extracellular osmolyte levels. A major challenge will be to clarify a possible link between L-carnitine and TRPV1 as well as transporters of L-carnitine.

Abbreviations

HCjE (human conjunctival epithelium); TRPV (transient receptor potential vanilloid); TRPM (transient receptor potential melastatin); CAP (capsaicin); CPZ (capsazepine); La^{3+} (lanthanum-III-chloride).

Acknowledgements

The authors thank Gabriele Fels for the technical assistance as well as Olaf Strauß (PhD) (both Charité, Dept. of Ophthalmology) for helpful discussions. In addition, the authors also thank Mathias Strowski (MD) and Carsten Grötzinger (PhD) from the Gastroenterology (Charité University Berlin) for their support and helpful discussions. Finally, the authors appreciate very much Friedrich Paulsen (MD) and Fabian Garreis (PhD) (University of Erlangen, Institute of Anatomy) for collaboration and for providing the IOBA-NHC cell line.

Stefan Mergler (PhD) is supported by DFG (Me 1706/13-1 and Me 1706/14-1) concerning TRP channel related research projects. Noushafarin Khajavi is supported by the DFG project of Stefan Mergler. The planar patch-clamp equipment was supported in part by Sonnenfeld-Stiftung (Berlin, Germany). Contract grant sponsor: Berliner Sonnenfeld-Stiftung. Contract grant number: 89745052.

References

1 Chen W, Zhang X, Li J, Wang Y, Chen Q, Hou C, Garrett Q: Efficacy of osmoprotectants on prevention and treatment of murine dry eye. Invest Ophthalmol Vis Sci 2013;54:6287-6297.
2 Xu S, Flanagan JL, Simmons PA, Vehige J, Willcox MD, Garrett Q: Transport of L-carnitine in human corneal and conjunctival epithelial cells. Mol Vis 2010;16:1823-1831.
3 Liedtke W: Role of TRPV ion channels in sensory transduction of osmotic stimuli in mammals. Exp Physiol 2007;92:507-512.
4 Mergler S, Garreis F, Sahlmuller M, Reinach PS, Paulsen F, Pleyer U: Thermosensitive transient receptor potential channels in human corneal epithelial cells. J Cell Physiol 2011;226:1828-1842.
5 Pan Z, Wang Z, Yang H, Zhang F, Reinach PS: TRPV1 activation is required for hypertonicity-stimulated inflammatory cytokine release in human corneal epithelial cells. Invest Ophthalmol Vis Sci 2011;52:485-493.
6 Ciura S, Bourque CW: Transient receptor potential vanilloid 1 is required for intrinsic osmoreception in organum vasculosum lamina terminalis neurons and for normal thirst responses to systemic hyperosmolality. J Neurosci 2006;26:9069-9075.
7 Mergler S, Garreis F, Sahlmuller M, Lyras EM, Reinach PS, Dwarakanath A, Paulsen F, Pleyer U: Calcium regulation by thermo- and osmosensing transient receptor potential vanilloid channels (TRPVs) in human conjunctival epithelial cells. Histochem Cell Biol 2012;137:743-761.
8 Grynkiewicz G, Poenie M, Tsien RY: A new generation of Ca2+ indicators with greatly improved fluorescence properties. J Biol Chem 1985;260:3440-3450.
9 Bruggemann A, Stoelzle S, George M, Behrends JC, Fertig N: Microchip technology for automated and parallel patch-clamp recording. Small 2006;2:840-846.
10 Mergler S, Skrzypski M, Sassek M, Pietrzak P, Pucci C, Wiedenmann B, Strowski MZ: Thermo-sensitive transient receptor potential vanilloid channel-1 regulates intracellular calcium and triggers chromogranin A secretion in pancreatic neuroendocrine BON-1 tumor cells. Cell Signal 2012;24:233-246.
11 Shamsi FA, Chaudhry IA, Boulton ME, Al-Rajhi AA: L-carnitine protects human retinal pigment epithelial cells from oxidative damage. Curr Eye Res 2007;32:575-584.

12 Corrales RM, Luo L, Chang EY, Pflugfelder SC: Effects of osmoprotectants on hyperosmolar stress in cultured human corneal epithelial cells. Cornea 2008;27:574-579.
13 Gavva NR, Tamir R, Klionsky L, Norman MH, Louis JC, Wild KD, Treanor JJ: Proton activation does not alter antagonist interaction with the capsaicin-binding pocket of TRPV1. Mol Pharmacol 2005;68:1524-1533.
14 Liu QY, Rosenberg RL: Activation and inhibition of reconstituted cardiac L-type calcium channels by palmitoyl-L-carnitine. Biochem Biophys Res Commun 1996;228:252-258.
15 Tewari K, Simard JM, Peng YB, Werrbach-Perez K, Perez-Polo JR: Acetyl-L-carnitine arginyl amide (ST857) increases calcium channel density in rat pheochromocytoma (PC12) cells. J Neurosci Res 1995;40:371-378.
16 Vriens J, Appendino G, Nilius B: Pharmacology of vanilloid transient receptor potential cation channels. Mol Pharmacol 2009;75:1262-1279.
17 Mergler S, Derckx R, Reinach PS, Garreis F, Bohm A, Schmelzer L, Skosyrski S, Ramesh N, Abdelmessih S, Polat OK, Khajavi N, Riechardt AI: Calcium regulation by temperature-sensitive transient receptor potential channels in human uveal melanoma cells. Cell Signal 2013;26:56-69.
18 Bron AJ, Tomlinson A, Foulks GN, Pepose JS, Baudouin C, Geerling G, Nichols KK, Lemp MA: Rethinking dry eye disease: a perspective on clinical implications. Ocul Surf 2014;12:S1-31.
19 Yang H, Wang Z, Capo-Aponte JE, Zhang F, Pan Z, Reinach PS: Epidermal growth factor receptor transactivation by the cannabinoid receptor (CB1) and transient receptor potential vanilloid 1 (TRPV1) induces differential responses in corneal epithelial cells. Exp Eye Res 2010;91:462-471.
20 Sumioka T, Okada Y, Reinach PS, Shirai K, Miyajima M, Yamanaka O, Saika S: Impairment of corneal epithelial wound healing in a TRPV1-deficient mouse. Invest Ophthalmol Vis Sci 2014;55:3295-3302.